RESEARCH PAPER | Science | Volume : 5 | Issue : 10 | October 2015 | ISSN - 2249-555X

The effect of firing temperature on the electrical properties and the microstructure of ZnO varistors doped with CuO

KEYWORDS: ZnO varistors, firing temperature, conductivity, dielectric constant and microstructure.

M.M.Saadeldin
Physics Department ,Faculty of Science, Cairo University, Giza/12613, Egypt

M.M.Younis
Micro Analytical Center ,Faculty of Science, Cairo University, Giza/12613, Egypt

M.M. Ahmed
Colonel engineer, Armed forces. Faculty member at the air defense collage, 12613, Egypt

M.Y. Helali
Assistant Researcher at the Space Research Laboratory - National Research Institute of Astronomy and Geophysics (NRIAG). Helwan, Cairo , 12613, Egypt

ABSTRACT *Mixtures of ZnO doped with CuO were prepared by solid state reaction from the calcined oxides. Additives present in grain boundaries between ZnO grains.XRD showed that no binary compound was formed and there are increase in dislocation density with additives. The conductivity and the dielectric constant are highly dependent on the microstructure of conducting grains surrounded by this insulating oxide barrier. Dielectric constant and conductivity are decreases where mixes fired at 1200°C. The amounts of additives affect the coefficient of non-linearity and breakdown voltage. Microstructure had been studied with SEM and AFM that revealed the presence of inter-granular phase. Increasing firing temperature increase the grain size of ZnO which doped with CuO.*

1.Introduction:

Varistors have wide spread applications in protecting power and signal level of electrical circuits against dangerous voltage surges(Levinson et al., 1986). This property is related to conduction mechanism in the inter- granular phase. Conduction mechanism is related to electronic structure in the vicinity of the grain boundaries. It is assumed that oxygen will be at ZnO grain boundaries. This oxygen is responsible for the generation of the electronic interface states out the grain boundaries . Schottky barriers are formed on both sides of the grain boundary where a depletion layer is formed as a result within the ZnO grains (Mahan et al., 1979).This depletion layer controls varistor action. Therefore ,conduction paths are located between grains in the region of closest contact over the Schottky barrier as well as through bulk inter-granular material at grain corners .The former may show a thermally activated temperature leakage conduction related to barrier height while the latter is thermally sensitive but is governed by different additives. (Nahm,2006) reported that the increase of sintering temperature led to more densified ceramics, whereas, it decreased the non-linear properties and varistor voltage. In view of this fact, the literature contains extensive reports describing the influence of processing variables on the properties and mechanisms that govern these system properties (Bernik and Daneu,2007 ;Cong et al.,2007 ; Park,2002 and Ott et al., 2001 (. Binary systems show non-linear coefficient of about [23-65] with maximum value for (4mol %). (Nahm,2012) also showed that the ceramics doped with 0.025 mol% Bi_{2O3} exhibited a surprisingly high nonlinear coefficient (α = 60) The aim of this paper is to study the effect of the addition of CuO and the firing at two different temperature on the electrical properties of ZnO varistors.

2.Materials and methods :

Sintered polycrystalline samples were prepared by conventional ceramic fabrication procedures. Reagent – grade ZnO, CuO , powders were mixed by wet ball – milling using deionized water. Disc specimens with the following dimensions ,diameter either 1.2cm and thickness 0.3 cm were processed under a force of 70 KN , dried and then fired at 900°C and 1200°C for 30 minutes . Specimens were first polished with different grades of diamond past thoroughly washed in an ultrasonic bath dried then ,thermally etched at 1000°C for 30 minutes as represented in table (1). Microstructure developed was examined under scanning electron microscope type FEI inspect S provided with EDAX ,after sputtering with gold .The (Hioki 3532 - 50 LCR HiTester) programmable automatic RCL meter was used for precise measurements of resistance, capacitance and inductance.

X-ray diffraction is a powerful non-destructive method for material characterization, by which the crystal structure, orientation, and grain size can be determined. The characterization is usually carried out with a typical X-ray wavelength that is comparable to the inter-atomic distance in a crystal. In terms of the path difference Δs, constructive interference occurs when Δs is an integral multiple of the wavelength λ. Thus scattered beams emerge only when the condition is met by a family of crystal planes, where m is an integer. This is the Bragg condition for diffraction. The intensity of the reflected beam has sharp peaks in the corresponding directions. They are called Bragg peaks. The Bragg peak can be found by varying the angle 2θ of the detector (Schwarzl et al., 2000)

$$2d \sin \theta = m\lambda \qquad (1)$$

The full width at half maximum (FWHM) of the peak, β (in radians), is a measure of the grain size (D), in a polycrystalline film, as described by Scherer's formula (Springholz G. et al., 2007):

$$D = \frac{0.89\lambda}{B \cdot COS(\theta)} \qquad (2)$$

Volume : 5 | Issue : 10 | October 2015 | ISSN - 2249-555X

Where θ is the Bragg angle. The starting materials namely; ZnO and CuO were examined by XRD. Using Philips apparatus type 170, a copper target (λ=1.54 Å) and Ni-filter. A continuous plot of intensity for 2Θ values 4 to 66 was made at a scanning speed of 1° / minute, with a paper speed of 10 mm/min. The dislocation cofficient (δ) of the samples can be determined from the following equation (Springholz G. et al., 2007):

$\delta = 1/D2$ (3)

The capacitance and resistance at frequency from 1 kHz to 2.5 MHz were measured at different temperatures between 300 to 550 K and the respective permittivity [ε`] and conductivity [σ] were calculated according to the following relations :

$\epsilon` = C.d/\epsilon_0 A$ (4)

C= Capacitance in Farad
d = thickness of specimen in m
ϵ_0= dielectric constant of vacuum = 8.85×10^{-12} F/m
A = area of specimen in m^2

Also , from the values of resistance [R] the resistivity [ρ] and conductivity[σ] were calculated from the following relation.

Resistivity [ρ] = RA/d
where R = resistance

Conductivity increase with increasing frequency in the frequency range up to 2.5 MHz. It is obvious that there are two slopes which refers to two mechanism of conduction and can be described by the following equation:

$\sigma = B\omega^s$ (5)

Where:

B: is constants.
s: is the frequency exponent factor.
ω: is angular frequency.

The value of (s) gives us informations about the specific mechanism of conduction involved.

By plotting the relation between lnσ and lnω we can easily calculate the slope and get (s) value.

3.Results and Discussion :
3.1. XRD results.
The XRD patterns of the respective mixes fired at 900^{0}C for 30 min , showed a shift in the d spacing equivalent to [0.03 – 0.04] A^0 in the main ZnO peak indicating a kind of limited solid solution of CuO in the oxide. A maximum shift of 0.04 A^0 was recorded in mix containing 6 mol % copper oxide , Figures (1) Show XRD results of compounds (M1, M2, M3, M4 and M5) respectively. The shift in ZnO peaks did not exceed the recorded value. Also table (2) show the grain size (D), interplanar distance (d) and the calculated dislocation(δ) for both samples at the different crystal orientations.

3.2. The electrical properties.
Figures (2) Shows the (I-V) Characteristic curve for sample M1 at both firing temperature. It is clear from the curves that there are decrease in the breakdown voltage where the firing temperature raised up to 1200^{0}C. (Sedky, 2012) As the sintering temperature increased, the breakdown field decreased over a wide range from 2838.7 to 6.41 V/cm, while the nonlinear coefficient is increased in the range of (23.86–47.76). Furthermore, the barrier height decreased from 1.76 to 0.974 eV. The highest value of non linearity coefficient was (68) for M4 that fired at 900^{0}C and contains 4mol% CuO.

Figures (3-a, b) Show The relation between conductivity (σ) and frequency at room temperature for group (I) fired at 900^{0}C and 1200^{0}C respectively. The results show increase in the conductivity as the frequency increase. Also comparison between conductivities of different compounds represent increase in values of (σ) by increasing concentration of additives reach to maximum value for mix (M4) which contain 4 mol% of CuO for both firing temperature. Also the firing at 900^{0}C has the higher conductivities than that achieved at 1200^{0}C.

Figures (4-a, b) represent the relation between lnσ and lnω. we can easily calculate the slope and get (s) value which refer to the type of conduction mechanism. The values of (s) is 0.89 for firing at 900^{0}C and 1.0 for firing at 1200^{0}C. According to earlier works in the nature of conduction mechanism that take place in ZnO varistors and according to the results that we have the (s) values gives us an indication that the conduction mechanism found to be agree with Correlated Barrier Hopping model (CBH).

Figures (5-a, b) show the relation between dielectric constant (ε`)and temperature at a frequency ( 100 k Hz ) for both firing temperature respectively. The observed dielectric constant of different mixtures was variably affected by increasing temperature from 298 to 533 K. Generally (ε`) appears to be slightly changed with rise of temperature and increases at the higher temperature ranges. Also the higher values were found to be achieved at the lower firing temperature. The increase of temperature raised the dielectric constant because it increases ionic response to the field again which is related to intergranular material at any particular frequency . Presumably these effects are associated with polarization currents arising from trapping states of various kinds and densities. In the ZnO - intergranular material interface, the states lying possibly in the transition region (interface) between ZnO and intergranular material. The variation of capacitance and resistance with temperature is thought to be associated with dielectric relaxation .

Figures (6-a and b) show the relation between conductivity and temperature at constant frequency (100 kHz) for both firing temperature respectively. Mixes behave differently according to the percentage of dopant added. Increasing the concentration of CuO leads to a gradual increase of σ as a function of temperature , due to the fact that , the increase of temperature activates the mobility of ions and increases the carrier density. This may be explained in the light of the microstructure formed at the semi-conductive ZnO grains surrounded by insulating glassy phase as a result the observed dielectric constant increased with increase in copper oxide. There are two models postulated to describe the microstructure of ZnO depending on constitution. A three phase model comprising grains , intergranular material and particles. And two model comprising the first two only. The addition of CuO leads to a two phase microstructure ; well crystalline ZnO grains showing grain growth in preferred orientation , ZnO crystallizes in hexagonal system, it is characterized by prefect cleavage plane along (001) which was distinct in SEM of ZnO with

Volume : 5 | Issue : 10 | October 2015 | ISSN - 2249-555X

different additives as shown by (Desouky,2011).

3.3.Microstructure analysis.
The SEM image of mix M3 fired at 900°C (fig.7) shows the surface morphology of the sample. The processing and additives play a great role in the shape of the surface morphology. The image represents a mass of solid solution of ZnO and CuO in some places are rich in (Zn) other in (Cu) which is shown as a kind of stereotions (dark and light lines), the mass is dissected by parallel cavities perpendicular to the lines of stereotions.

Microstructure of ZnO ceramics play an important role in the electric characteristic displayed. There are two models postulated to describe the microstructure of ZnO depending on the constitution.

Wet – SPM (Scanning Probe microscope), Shimadzu made in Japan is used to study the surface and the microstructure of different samples by the non contact mode. Figure (8-a) shows the AFM plane image for sample M1 at both firing temperature scan range for a single scan is 10μm x 10μm which represent Large-quantity growth of hexagonal prismatic ZnO with CuO. The image shows a polycrystalline structure with intergranular spacing between each other. Figure (8-b) shows the three dimensional image for the same mixes with heights from 0 nm at the darkest places and max. height of about 771.14 nm at the brightest places and from 0 nm to 1.21 μm respectively. AFM data can generate quantitative information from individual particles and between groups of particles. Figure (8-c) and table (4-a,b) show their particles analyses which are maximum diameter, mean radius, perimeter, surface area, volume, distortion and roughness for each particle. This data represent that the max. diameter of the smallest grain was 0.262 μm with surface roughness of 1.05 and the max. diameter of the largest one was 2.474 μm with surface roughness of 2.739 for sample M1 fired at 900°C, And that for the same sample where fired at 1200°C are 0.431 μm and surface roughness 1.148 for the smallest grain and 3.125 μm with roughness 2.3 for the largest one. The comparisons between the average grain size for both samples represents that there are increase in the grain size by increasing the firing temperature. The average values of (mean radius, maximum diameter, distortion coefficient, volume and roughness) for mixes M1/900°C and M1/1200°C are shown in table(5).

4.Conclusion:
XRD showed that no binary compound was formed and there are decrease in grain size and increase in dislocation density due to the additives.

The BDV has lower values where samples fired at 1200°C.

The conductivity and the dielectric constant are highly dependent on the microstructure of conducting grains surrounded by this insulating oxide barrier.

Conduction mechanism found to be agree with Correlated Barrier Hopping model (CBH).

Dielectric constant and conductivity are decreases where mixes fired at 1200°C

SEM and AFM revealed the presence of inter-granular phase. Additives present in grain boundaries between ZnO grains.

Increasing firing temperature increase the grain size of ZnO which doped with CuO.

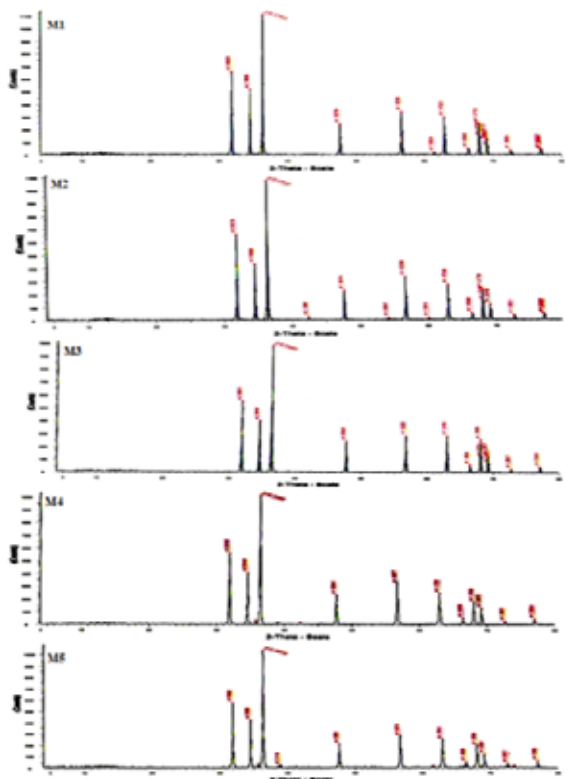

Fig.(1) XRD of group (I) (ZnO+CuO)

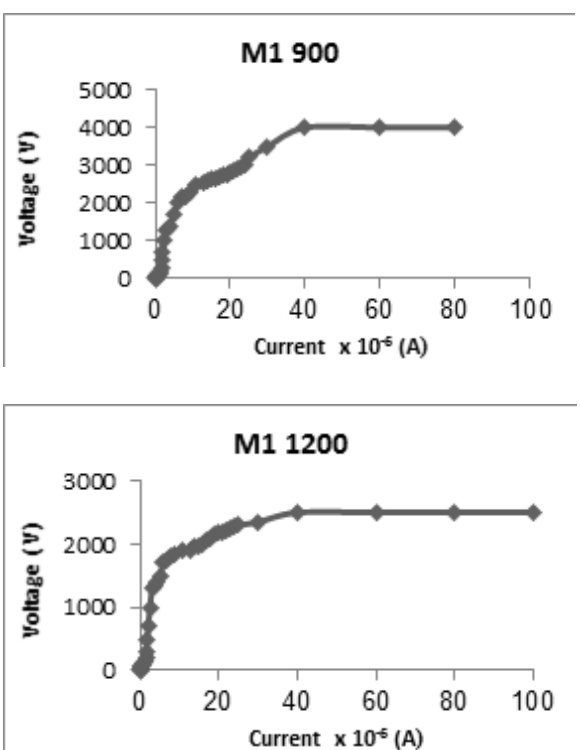

Fig.(2): (I-V) Characteristics of M1 (ZnO – CuO)/900°C &1200°C.

Volume : 5 | Issue : 10 | October 2015 | ISSN - 2249-555X

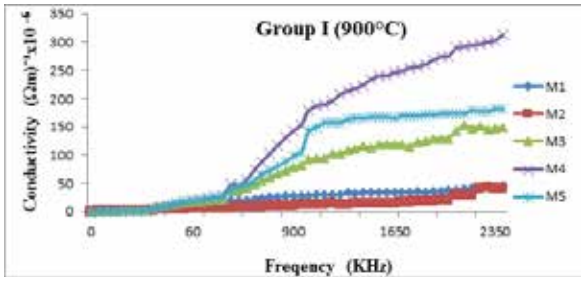

Fig.(3-a):The relation between dielectric Conductivity(σ) and frequency at room temperature for group I/900°C.

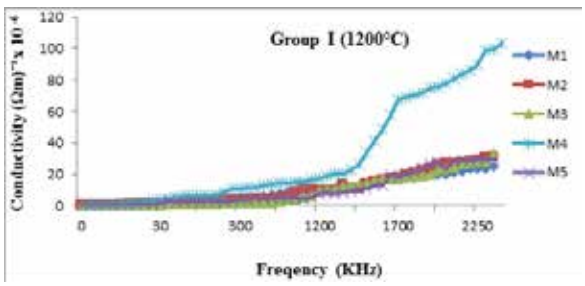

Fig.(3-b) The relation between dielectric Conductivity(σ) and frequency at room temperature for group I/1200°C.

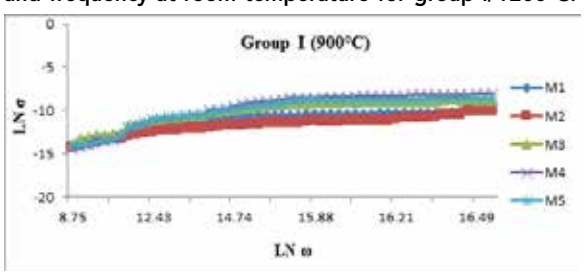

Fig.(4-a): The relation between LN σ and LN ω at room temperature for group I/900°C.

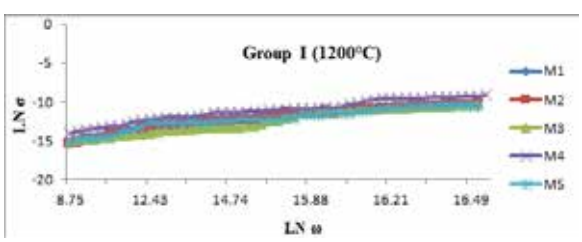

Fig.(4-b): The relation between LN σ and LN ω at room temperature for group I/1200°C.

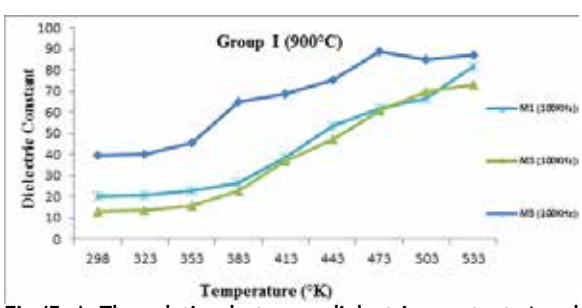

Fig.(5-a): The relation between dielectric constant ε′ and temperature at 100 KHz for group I/900°C.

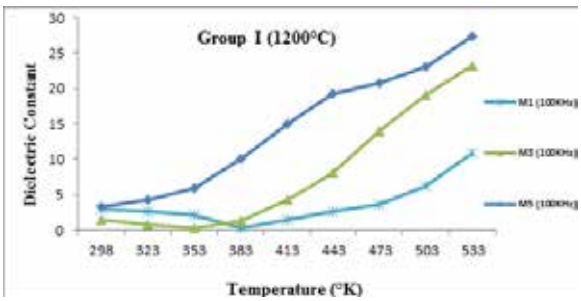

Fig.(5-b): The relation between dielectric constant ε′ and temperature at 100 KHz for group I/1200°C

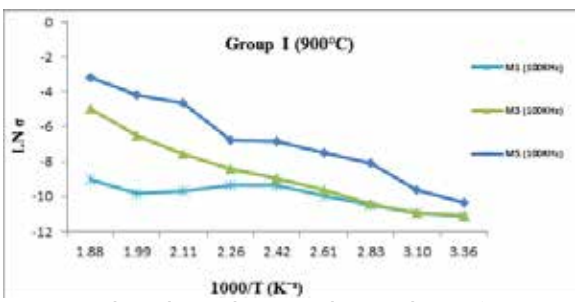

Fig.(6-a): The relation between ln σ and 1000/T at constant frequency 100 KHz for group I/900°C.

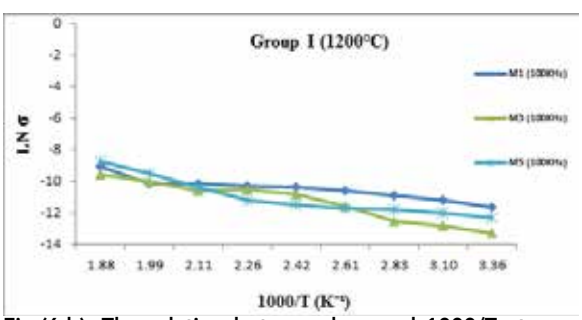

Fig.(6-b): The relation between ln σ and 1000/T at constant frequency 100 KHz for group I/1200°C.

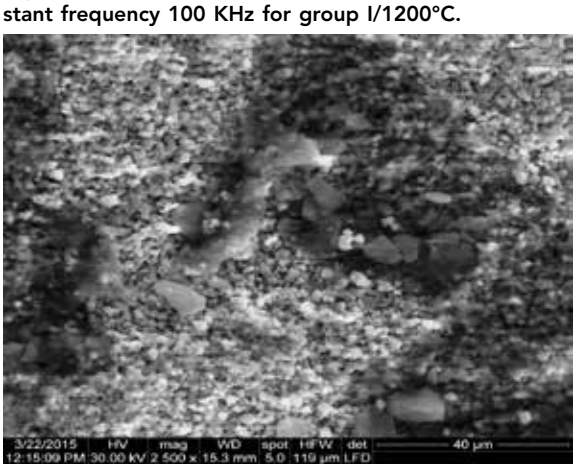

Fig.(7): SEM of group I, sample M3/900°C, X=2000.

Volume : 5 | Issue : 10 | October 2015 | ISSN - 2249-555X

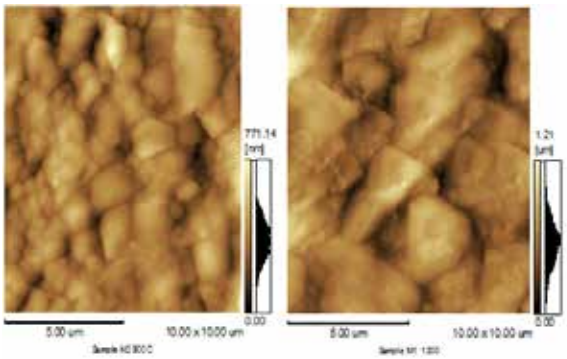

Fig.(8-a) AFM plane image for sample M1/900°C &1200°C.

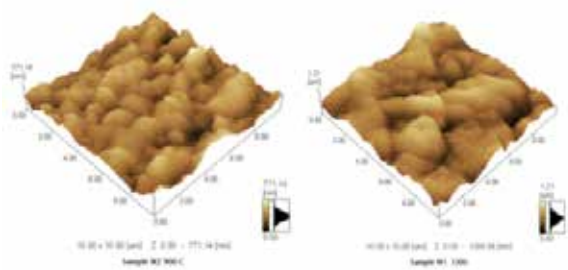

Fig.(8-b)AFM 3D image for sample M1/900°C &1200°C..

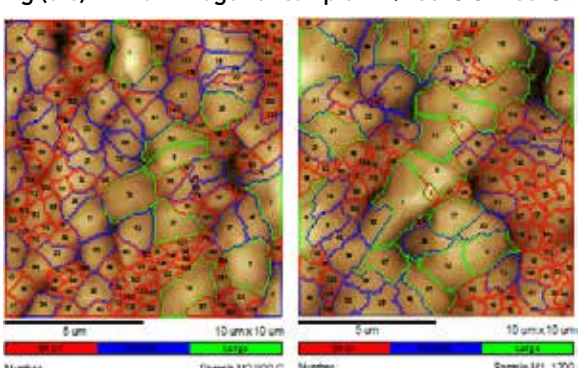

Fig.(8-c)AFM particle analyses image for sample M1 /900°C &1200°C..

OXIDES		ZnO mol%	CuO mol%
GROUP (I)	M1	99.5	0.5
	M2	99	1
	M3	98	2
	M4	96	4
	M5	94	6

Table (1): Composition of different mixes in mol%.

%CuO content	α 900°C	α 1200 °C
0.5	30.1	39.2
1	47.7	45.9
2	56	48.8
4	68.1	45.2
6	24.3	25.7

Table (2): The non linearity of group I.

S	hkl	2Θ	d(A°)	Crystal size (nm)	Dislocation(δ) x10^{-5} (nm)
M1	100	31.76243	2.808	205.9	2.36
	002	34.44082	2.595	232	1.86
	101	36.25219	2.470	219.9	2.07
	102	47.55215	1.907	172.7	3.35
	110	56.57493	1.623	183.9	2.96
	103	62.87885	1.475	177.2	3.18
	200	66.34905	1.4066	227	1.94
	112	67.93824	1.3777	196.4	2.59
	201	69.05728	1.357	243.9	1.68
	004	72.6212	13005	197.2	2.57
	202	76.94449	1.2344	232.5	1.85
M2	100	31.73488	2.807	193.3	2.68
	002	34.42162	2.969	226.4	1.95
	101	36.57311	2.470	173.6	3.32
	102	47.52382	1.9074	183	2.99
	110	56.54103	1.623	185.5	2.91
	103	62.84706	1.475	155.5	4.14
	200	66.31263	1.405	186.3	2.88
	112	67.9884	1.377	180.9	3.06
	201	69.03972	1.3576	211.1	2.24
	004	72.5676	1.3005	174.3	3.29
	202	76.90795	1.225	193.3	2.68
M3	100	31.75277	2.8021	238.1	1.76
	002	34.39997	2.591	200.8	2.48
	101	36.22594	2.4666	213.7	2.19
	102	47.51447	1.905	190.6	2.75
	110	56.56822	1.6220	200.5	2.49
	103	62.85999	1.474	164.8	3.68
	200	66.35193	1.405	131.4	5.79
	112	67.91151	1.376	205.4	2.37
	201	69.06156	1.357	280.5	1.27
	004	72.55544	1.2993	255.7	1.53
	202	76.91807	1.236	190.8	2.75
M4	100	31.79772	2.8018	187.7	2.84
	002	34.4677	2.59149	196.2	2.6
	101	36.28671	2.4650	193.8	2.66
	102	47.57511	1.9044	175.4	3.25
	110	56.61388	1.6207	182.5	3
	103	62.89518	1.4733	152.6	4.29
	200	66.37368	1.404	139	5.18
	112	67.9672	1.3753	166.7	3.6
	201	69.09251	1.3557	193.1	2.68
	004	72.61215	1.298	108.5	8.49
	202	76.97253	1.2355	124	6.5
M5	100	31.74402	2.806	235.6	1.8
	002	34.41916	2.5966	217.5	2.11
	101	36.23222	2.469	205.5	2.37
	102	47.51894	1.906	196.4	2.59
	110	56.55813	1.622	178.7	3.13
	103	62.84645	1.4744	218.4	2.1
	200	66.3245	1.4055	161	3.86
	112	67.91952	1.376	243	1.69
	201	69.04477	1.3568	239	1.75
	004	72.59021	1.3001	210.3	2.26
	202	76.92967	1.236	139.5	5.14

Table(3):The structural parameters of group I (ZnO + CuO).

Volume : 5 | Issue : 10 | October 2015 | ISSN - 2249-555X

No.	Class	Maximum Diameter [µm]	Mean Radius [µm]	Perimeter [µm]	Surface Area [µm2]	Volume [nm3]	Distortion	Roughness
1	Large	2.236	0.893	6.927	3.196	1.14E+09	0.799	1.553
2	Mediam	2.061	0.661	5.2	1.247	4.29E+08	0.424	2.038
3	Large	2.248	0.744	6.337	1.636	6.45E+08	0.616	2.182
4	Mediam	1.836	0.54	4.591	0.722	2.92E+08	0.372	2.476
5	Small	1.313	0.497	3.717	0.806	3.52E+08	0.995	1.523
6	Mediam	2.163	0.646	5.146	1.25	4.56E+08	0.437	1.934
7	Large	1.99	0.843	6.342	2.541	9.55E+08	0.991	1.405
8	Large	2.369	0.744	5.919	1.584	5.78E+08	0.405	2.015
9	Mediam	2.191	0.694	5.592	1.464	5.98E+08	0.515	1.855
10	Small	0.758	0.31	2.273	0.386	1.57E+08	0.985	1.283
11	Mediam	1.734	0.675	5.089	1.625	5.95E+08	0.971	1.42
12	Small	1.061	0.393	2.839	0.558	2.53E+08	0.691	1.251
13	Mediam	1.658	0.608	4.877	1.347	4.48E+08	0.967	1.641
14	Small	0.891	0.365	2.627	0.483	2.16E+08	0.996	1.233
15	Mediam	2.067	0.62	5.373	1.02	4.67E+08	0.379	2.393
16	Large	2.657	0.912	7.594	2.475	9.38E+08	0.932	1.964
17	Mediam	1.792	0.65	5.277	1.401	4.75E+08	0.761	1.709
18	Small	1.139	0.351	2.69	0.417	1.43E+08	0.368	1.685
19	Small	0.984	0.396	3.014	0.588	2.26E+08	1	1.41
20	Mediam	1.493	0.505	3.837	0.686	2.76E+08	0.822	1.873
21	Mediam	1.725	0.581	5.111	0.956	4.23E+08	0.63	2.279
22	Mediam	1.466	0.632	4.43	1.463	5.09E+08	0.9	1.221
23	Small	0.902	0.334	2.576	0.365	1.48E+08	0.849	1.559
24	Mediam	2.313	0.636	5.815	0.687	2.64E+08	0.205	4.188
25	Mediam	1.391	0.565	4.696	1.083	4.6E+08	0.9	1.694
26	Small	1.632	0.445	3.485	0.414	1.47E+08	0.4	2.815
27	Large	2.067	0.746	6.159	1.79	6.7E+08	0.764	1.797
28	Mediam	1.611	0.595	4.74	1.188	4.53E+08	0.802	1.634
29	Small	1.657	0.449	3.767	0.418	1.92E+08	0.216	2.782
30	Small	1.26	0.387	3.151	0.454	1.64E+08	0.439	1.94
31	Mediam	1.829	0.666	5.673	1.523	5.26E+08	0.764	1.923
32	Small	1.196	0.455	3.532	0.757	2.54E+08	0.995	1.482
33	Mediam	1.68	0.598	5.125	1.163	4E+08	0.937	1.974
34	Small	0.704	0.259	1.959	0.271	86293287	0.586	1.419
35	Large	1.843	0.701	5.515	1.675	6.63E+08	0.726	1.572
36	Mediam	1.776	0.625	5.388	1.192	4.57E+08	0.917	2.057
37	Small	0.845	0.346	2.525	0.444	1.46E+08	0.964	1.298
38	Mediam	2.248	0.683	6.159	0.969	3.62E+08	0.329	3.292
39	Mediam	1.486	0.512	3.98	0.88	3.44E+08	0.607	1.547
40	Small	1.36	0.473	3.726	0.799	2.51E+08	0.995	1.712
41	Mediam	1.459	0.585	4.334	1.178	4.43E+08	0.911	1.368
42	Small	1.445	0.433	3.536	0.459	1.89E+08	0.43	2.304
43	Mediam	1.507	0.642	4.719	1.432	5.04E+08	0.972	1.347
44	Small	1.034	0.42	2.936	0.656	2.09E+08	0.944	1.18
45	Mediam	1.359	0.501	4.016	0.827	2.81E+08	0.805	1.71
46	Small	1.272	0.496	3.677	0.887	2.82E+08	0.962	1.351
47	Mediam	1.872	0.626	5.212	1.241	4.38E+08	0.855	1.847
48	Mediam	1.528	0.529	4.776	0.851	2.89E+08	0.999	2.297
49	Small	1.1	0.417	3.014	0.614	2.14E+08	0.758	1.284
50	Large	2.474	0.76	6.693	1.427	4.66E+08	0.435	2.739
51	Small	0.863	0.307	2.429	0.372	93998597	0.667	1.628
52	Mediam	1.466	0.553	4.056	1.03	3.31E+08	0.943	1.388
53	Small	1.175	0.421	3.46	0.62	2.29E+08	0.927	1.669
54	Mediam	1.56	0.509	3.988	0.919	2.79E+08	0.709	1.623
55	Mediam	1.415	0.583	4.26	1.206	3.64E+08	0.941	1.35
56	Small	1.258	0.454	3.317	0.668	2.45E+08	0.988	1.396
57	Small	1.154	0.406	3.003	0.547	1.92E+08	0.677	1.404
58	Small	1.052	0.39	3.027	0.553	1.93E+08	0.986	1.457
59	Small	0.699	0.29	2.046	0.304	1.1E+08	0.774	1.193
60	Small	1.088	0.385	3.281	0.497	1.83E+08	0.571	1.852
61	Small	1.226	0.415	3.193	0.616	1.7E+08	0.601	1.573
62	Small	1.157	0.422	3.157	0.599	2.22E+08	0.702	1.428
63	Mediam	1.458	0.517	4.14	0.889	2.8E+08	0.655	1.643
64	Mediam	1.507	0.545	4.237	0.935	3.1E+08	0.861	1.654
65	Small	1.058	0.369	2.774	0.469	1.7E+08	0.647	1.403
66	Mediam	2.313	0.61	6.331	0.886	3.14E+08	0.281	3.766
67	Small	0.989	0.359	2.644	0.458	1.6E+08	0.647	1.361
68	Small	0.906	0.373	2.678	0.505	1.64E+08	1	1.256
69	Small	0.858	0.297	2.383	0.28	84171509	0.558	1.795
70	Small	0.699	0.271	2.029	0.274	91825666	0.906	1.342
71	Mediam	1.744	0.577	4.304	1.053	3.2E+08	0.483	1.517
72	Large	2.278	0.876	6.624	2.511	8.3E+08	0.865	1.473
73	Small	0.737	0.222	1.84	0.141	54644263	0.452	2.007

Volume : 5 | Issue : 10 | October 2015 | ISSN - 2249-555X

74	Small	0.821	0.271	1.997	0.265	97020677	0.528	1.291
75	Small	0.845	0.311	2.452	0.326	1.26E+08	0.897	1.537
76	Small	0.758	0.262	1.97	0.22	73915879	0.976	1.521
77	Small	1.255	0.486	3.736	0.861	2.33E+08	0.743	1.532
78	Mediam	1.702	0.567	4.679	0.878	2.78E+08	0.918	2.114
79	Small	0.483	0.174	1.265	0.114	44598828	0.719	1.192
80	Small	1.025	0.297	2.715	0.233	84693470	0.386	2.615
81	Small	0.276	0.103	0.722	0.043	18751199	0.634	0.971
82	Small	0.393	0.152	1.054	0.088	33746922	0.714	1.092
83	Small	1.454	0.477	3.961	0.743	2.18E+08	0.544	1.881
84	Small	1.141	0.361	2.991	0.343	1.23E+08	0.754	2.18
85	Small	0.797	0.266	1.997	0.241	88677832	0.584	1.424
86	Small	0.577	0.203	1.477	0.149	51996179	0.731	1.292
87	Small	0.47	0.172	1.252	0.116	40798268	0.763	1.167
88	Mediam	1.495	0.524	3.947	0.86	2.86E+08	0.848	1.545
89	Small	1.094	0.35	2.677	0.357	1.11E+08	0.432	1.73
90	Small	0.77	0.237	1.877	0.178	65528667	0.604	1.64
91	Mediam	1.669	0.677	5.378	1.565	4.92E+08	0.987	1.55
92	Small	1.031	0.366	2.802	0.397	1.41E+08	0.875	1.638
93	Mediam	1.437	0.502	4.399	0.791	2.69E+08	0.986	2.064
94	Small	0.674	0.216	1.6	0.149	56254135	0.452	1.406
95	Small	0.97	0.359	2.622	0.483	1.3E+08	0.953	1.332
96	Small	1.004	0.363	2.835	0.417	1.38E+08	0.993	1.65
97	Small	1.028	0.358	2.709	0.412	1.24E+08	0.608	1.513
98	Small	0.524	0.217	1.518	0.193	59589057	1	1.124
99	Small	0.647	0.264	2.139	0.258	91520993	0.909	1.52
100	Mediam	1.298	0.5	3.555	0.873	2.82E+08	0.668	1.241
101	Small	1.602	0.455	3.932	0.452	1.62E+08	0.267	2.771
102	Small	0.829	0.234	1.839	0.122	42085386	0.18	2.383
103	Small	1.436	0.463	4.504	0.627	2.18E+08	0.678	2.665
104	Small	0.408	0.156	1.164	0.09	36393013	0.806	1.218
105	Small	0.891	0.258	2.025	0.1	38303248	0.954	3.29
106	Small	0.591	0.216	1.629	0.166	63297168	0.707	1.305
107	Small	0.262	0.089	0.634	0.031	12710899	0.534	1.05
108	Small	0.587	0.218	1.646	0.168	57907475	0.709	1.346
109	Small	0.829	0.279	2.162	0.304	91843747	0.552	1.418
110	Small	0.456	0.169	1.141	0.097	32574050	0.998	1.132
111	Small	0.514	0.183	1.339	0.125	44490023	0.865	1.199
112	Small	0.751	0.261	1.922	0.263	80722592	0.838	1.276
113	Small	0.563	0.24	1.73	0.221	74315011	0.958	1.156
114	Small	0.664	0.259	1.909	0.228	74714916	0.904	1.358
115	Small	0.892	0.307	2.351	0.338	83726861	0.986	1.471
116	Small	1.063	0.364	2.791	0.444	1.24E+08	0.504	1.483
117	Small	0.727	0.222	1.661	0.123	37352907	0.741	2.056
118	Small	1.458	0.499	4.026	0.715	1.86E+08	0.539	1.97
119	Small	0.845	0.313	2.277	0.358	94508905	0.718	1.293
120	Small	0.977	0.399	2.93	0.555	1.63E+08	0.95	1.298
121	Small	0.591	0.22	1.541	0.182	54246459	0.749	1.147
122	Small	0.36	0.119	0.855	0.051	18440942	0.471	1.156
123	Small	1.477	0.479	3.786	0.662	1.92E+08	0.709	1.759
124	Small	0.83	0.243	1.951	0.119	39875128	0.627	2.612
125	Small	0.998	0.351	2.608	0.409	1.02E+08	0.711	1.448
126	Small	0.853	0.299	2.203	0.319	82218954	0.551	1.332
127	Small	0.36	0.138	1.099	0.066	23061707	0.976	1.466
128	Small	0.919	0.326	2.595	0.364	1.04E+08	0.899	1.596
129	Small	0.824	0.253	1.932	0.186	56483685	0.962	1.664
130	Small	0.683	0.292	2.056	0.314	87722068	1	1.148
131	Small	0.683	0.22	1.821	0.158	43223714	0.838	1.784
132	Small	0.813	0.306	2.212	0.331	89814920	0.979	1.257
133	Small	0.695	0.229	1.776	0.16	50564993	0.987	1.596
134	Small	0.437	0.178	1.297	0.114	35907141	0.95	1.219
135	Small	0.595	0.202	1.477	0.147	40639836	0.725	1.292
136	Small	0.385	0.15	1.04	0.082	26472309	0.998	1.085
137	Small	0.644	0.245	1.827	0.191	61541002	1	1.427
138	Small	1.154	0.369	2.892	0.386	1.18E+08	0.57	1.766
139	Small	0.734	0.283	2.12	0.285	87533364	0.86	1.303
140	Small	0.767	0.306	2.305	0.34	94680373	0.859	1.307
141	Small	0.349	0.123	0.897	0.054	17835384	0.994	1.2
142	Small	0.695	0.232	1.743	0.18	52698100	0.99	1.403
143	Small	0.393	0.127	0.924	0.052	16149330	0.31	1.35
144	Small	0.977	0.375	2.94	0.492	1.29E+08	0.843	1.468
145	Small	0.707	0.221	1.656	0.149	41987138	0.467	1.537
146	Small	0.531	0.18	1.307	0.105	26699633	0.903	1.414
147	Small	0.813	0.298	2.296	0.285	82070361	0.963	1.519
148	Small	0.591	0.215	1.716	0.157	43925078	0.794	1.568
149	Small	0.514	0.186	1.454	0.135	34950694	0.857	1.361

Volume : 5 | Issue : 10 | October 2015 | ISSN - 2249-555X

150	Small	0.431	0.151	1.067	0.086	25904133	0.514	1.079
151	Small	1.019	0.37	2.879	0.448	1.19E+08	0.679	1.527
152	Small	0.437	0.138	1.164	0.049	14330412	0.444	2.208
153	Small	0.791	0.258	1.896	0.202	50724879	0.931	1.511
154	Small	0.618	0.244	1.753	0.216	53753333	0.859	1.205
155	Small	0.587	0.23	1.739	0.189	48706664	0.958	1.372
156	Small	0.845	0.312	2.212	0.354	81139285	0.94	1.198
157	Small	0.595	0.208	1.495	0.146	38998364	0.769	1.268
158	Small	0.641	0.21	1.629	0.127	32905799	0.984	1.73
159	Small	0.631	0.241	1.863	0.209	51042534	0.752	1.403
160	Small	0.631	0.24	1.724	0.213	45750029	0.645	1.202
161	Small	1.105	0.437	3.505	0.658	1.52E+08	0.702	1.563
162	Small	0.863	0.259	2.134	0.168	39914431	0.323	2.24
163	Small	0.631	0.265	1.808	0.261	58562982	0.984	1.079
164	Small	0.581	0.225	1.707	0.184	47700968	0.706	1.321
165	Small	0.334	0.102	0.791	0.034	9432875	0.484	1.482
166	Small	0.704	0.207	1.61	0.12	32787549	0.374	1.733
167	Small	0.72	0.314	2.117	0.353	80906628	0.997	1.067
168	Small	0.161	0.072	0.455	0.023	5805811	0.839	0.721
169	Small	0.591	0.195	1.578	0.132	28696913	0.492	1.527
170	Small	0.402	0.155	1.086	0.091	18239777	0.948	1.079
171	Small	0.315	0.124	0.865	0.062	10252183	0.741	1

Table(4-a):AFM particle analyses for sample M1/900°C.

No.	Class	Maximum Diameter [µm]	Mean Radius [µm]	Perimeter [µm]	Surface Area [µm2]	Volume [nm3]	Distortion	Roughness
1	Large	2.606	1.001	9.071	3.703	2.252	0.881	2.163
2	Small	1.154	0.369	2.932	0.479	0.234	0.952	2.359
3	Large	3.091	1.052	10.11	4.357	1.939	0.686	2.473
4	Large	2.835	0.801	7.503	1.286	0.824	0.248	4.254
5	Mediam	1.766	0.604	4.744	1.296	0.728	0.867	1.726
6	Large	2.397	0.768	7.114	2.177	1.228	0.734	2.428
7	Small	1.206	0.41	3.442	0.608	0.377	0.974	2.013
8	Mediam	1.851	0.633	5.432	1.555	0.731	0.602	1.9
9	Large	2.041	0.777	6.395	2.108	1.094	0.725	1.847
10	Large	2.026	0.774	6.616	2.167	1.186	0.861	1.912
11	Large	1.95	0.754	6.23	2.11	1.14	0.997	1.739
12	Large	3.125	1.012	8.672	3.038	1.728	0.619	2.3
13	Small	0.954	0.268	2.204	0.164	0.116	0.937	2.639
14	Mediam	1.758	0.604	4.652	1.255	0.642	0.974	1.638
15	Large	2.884	1.022	9.04	3.404	1.669	0.703	2.24
16	Small	0.618	0.221	1.629	0.215	0.129	0.867	1.281
17	Large	2.068	0.729	5.647	2.193	1.152	0.667	1.542
18	Small	1.336	0.405	3.515	0.483	0.295	0.956	2.352
19	Large	2.789	0.885	8.199	2.156	1.068	0.501	2.772
20	Small	1.705	0.468	4.109	0.382	0.256	0.317	3.879
21	Mediam	2.102	0.675	5.534	1.374	0.925	0.999	1.953
22	Mediam	1.74	0.598	5.089	1.168	0.635	0.745	2.081
23	Mediam	1.824	0.595	4.864	1.184	0.64	0.488	1.919
24	Large	2.393	0.799	7.249	2.202	1.015	0.645	2.385
25	Mediam	1.914	0.644	5.998	1.139	0.696	0.801	2.68
26	Mediam	1.985	0.67	5.862	1.503	0.595	0.546	2.101
27	Large	2.505	0.785	6.942	1.871	1.17	0.717	2.277
28	Large	2.286	0.728	5.647	1.881	0.749	0.655	1.708
29	Small	1.206	0.42	4.039	0.725	0.386	0.95	2.21
30	Small	1.265	0.492	3.81	1.062	0.465	0.773	1.479
31	Mediam	1.672	0.547	4.338	0.964	0.525	0.954	1.841
32	Small	1.26	0.472	4.13	0.763	0.472	0.999	2.031
33	Small	1.756	0.498	4.3	0.427	0.244	0.487	3.92
34	Small	1.001	0.34	2.553	0.358	0.266	0.929	1.491
35	Mediam	1.322	0.545	4.265	1.328	0.545	0.994	1.509
36	Small	0.786	0.283	2.263	0.383	0.166	0.744	1.581
37	Small	1.196	0.418	3.441	0.654	0.343	0.894	1.71
38	Small	0.598	0.235	1.707	0.242	0.123	0.857	1.216
39	Small	1.213	0.406	4.012	0.476	0.28	0.679	3.109
40	Mediam	1.474	0.556	4.369	1.117	0.526	0.755	1.546
41	Mediam	1.519	0.526	4.159	0.942	0.511	1	1.689
42	Mediam	1.606	0.525	4.288	0.886	0.426	0.79	1.998
43	Small	1.004	0.415	3	0.699	0.29	0.986	1.297
44	Small	0.746	0.234	1.896	0.153	0.11	0.639	1.912
45	Small	1.172	0.415	3.532	0.577	0.323	0.822	2.008
46	Small	0.884	0.334	2.42	0.463	0.209	0.852	1.305
47	Large	2.439	0.808	6.805	1.886	0.885	1	2.214
48	Mediam	1.735	0.591	5.111	1.04	0.582	0.995	2.234

Volume : 5 | Issue : 10 | October 2015 | ISSN - 2249-555X

49	Small	0.758	0.287	2.176	0.32	0.161	0.999	1.435
50	Large	1.922	0.756	6.057	2.173	0.96	0.87	1.601
51	Small	0.835	0.276	2.056	0.243	0.139	0.484	1.531
52	Mediam	1.503	0.567	4.464	1.207	0.542	0.937	1.584
53	Small	0.805	0.256	2.033	0.217	0.123	0.447	1.71
54	Mediam	1.632	0.614	4.652	1.311	0.704	0.974	1.46
55	Small	0.891	0.351	3.018	0.428	0.24	0.769	1.892
56	Small	0.929	0.317	2.471	0.434	0.165	0.684	1.568
57	Small	0.891	0.294	2.305	0.288	0.147	0.967	1.732
58	Mediam	1.381	0.557	4.426	1.132	0.532	0.849	1.557
59	Small	0.514	0.203	1.454	0.164	0.095	0.745	1.148
60	Mediam	1.536	0.513	4.288	0.831	0.462	0.512	1.961
61	Small	0.699	0.28	2.199	0.31	0.174	0.785	1.408
62	Small	0.758	0.26	1.983	0.268	0.131	0.592	1.415
63	Mediam	1.535	0.525	4.397	1.124	0.423	0.687	1.91
64	Mediam	1.662	0.501	4.641	0.621	0.276	0.56	3.265
65	Small	1.025	0.319	2.525	0.342	0.178	0.408	1.704
66	Small	1.272	0.477	3.957	0.866	0.383	0.772	1.73
67	Large	2.006	0.71	5.797	1.641	0.767	0.653	1.831
68	Mediam	1.946	0.565	4.692	0.808	0.423	0.623	2.428
69	Mediam	1.611	0.535	4.675	0.872	0.438	0.623	2.266
70	Small	0.906	0.288	2.322	0.245	0.15	0.485	1.839
71	Small	0.611	0.205	1.545	0.183	0.073	0.616	1.399
72	Mediam	1.713	0.597	4.656	1.218	0.491	0.992	1.631
73	Small	1.04	0.378	3.294	0.521	0.264	0.832	1.886
74	Mediam	2.002	0.597	5.152	0.728	0.339	0.449	3.103
75	Small	1.031	0.281	2.701	0.195	0.094	0.353	3.368
76	Small	0.781	0.309	2.484	0.378	0.193	0.973	1.497
77	Mediam	1.658	0.691	5.207	1.867	0.68	0.992	1.413
78	Small	1.013	0.375	2.806	0.523	0.218	0.835	1.392
79	Small	1.022	0.332	2.525	0.373	0.184	0.435	1.525
80	Mediam	1.464	0.533	3.98	1.034	0.385	0.844	1.467
81	Small	1.004	0.381	3.022	0.484	0.258	0.56	1.598
82	Small	0.816	0.304	2.517	0.358	0.189	0.903	1.551
83	Small	0.865	0.326	2.654	0.373	0.212	0.604	1.604
84	Mediam	2.064	0.641	5.681	1.069	0.411	0.399	2.764
85	Small	1.682	0.486	4.426	0.403	0.204	0.383	4.022
86	Small	0.892	0.284	2.208	0.251	0.11	0.821	1.791
87	Small	1.139	0.393	3.041	0.535	0.224	0.716	1.555
88	Small	1.258	0.443	3.58	0.714	0.315	0.868	1.736
89	Small	1.301	0.474	4.149	0.755	0.303	1	2.041
90	Small	1.251	0.417	3.178	0.583	0.246	0.535	1.733
91	Small	0.881	0.303	2.627	0.34	0.156	0.672	1.846
92	Small	1.349	0.435	3.61	0.684	0.262	0.4	1.888
93	Mediam	1.548	0.546	4.247	1.098	0.406	0.639	1.583
94	Small	0.626	0.275	1.951	0.386	0.128	0.952	1.174
95	Mediam	1.723	0.592	5.001	1.084	0.456	0.905	2.17
96	Small	0.489	0.155	1.307	0.085	0.037	1	1.895
97	Small	1.306	0.35	2.926	0.236	0.111	0.894	3.167
98	Small	0.824	0.351	2.705	0.556	0.182	0.984	1.414
99	Small	1.067	0.449	3.386	0.709	0.306	0.921	1.413
100	Small	1.014	0.326	2.894	0.32	0.134	0.74	2.496
101	Small	1.172	0.458	3.791	0.772	0.291	0.905	1.64
102	Small	1.111	0.415	3.349	0.582	0.284	0.606	1.648
103	Small	0.598	0.224	1.821	0.161	0.088	0.801	1.68
104	Small	0.569	0.235	1.697	0.266	0.095	0.839	1.183
105	Small	0.816	0.247	2.185	0.185	0.088	0.391	2.264
106	Small	0.785	0.281	2.157	0.264	0.133	0.589	1.479
107	Small	0.95	0.352	2.783	0.465	0.176	0.668	1.542
108	Small	0.769	0.229	1.873	0.168	0.058	0.459	2.152
109	Small	0.892	0.355	2.839	0.512	0.164	0.786	1.58
110	Small	0.63	0.231	1.753	0.193	0.096	0.661	1.335
111	Small	0.596	0.192	1.398	0.141	0.052	0.639	1.378
112	Small	1.602	0.49	4.279	0.714	0.273	0.575	2.221
113	Small	0.477	0.183	1.421	0.142	0.052	0.999	1.386
114	Small	1.212	0.477	3.745	0.832	0.344	1	1.505
115	Small	0.445	0.163	1.206	0.117	0.04	0.971	1.33
116	Mediam	1.454	0.501	4.071	0.873	0.299	0.954	1.801
117	Small	1.094	0.382	3.285	0.504	0.184	0.739	1.988
118	Small	0.929	0.373	3.069	0.581	0.192	0.794	1.616
119	Small	0.431	0.165	1.196	0.122	0.045	0.752	1.148
120	Small	0.902	0.332	2.503	0.4	0.159	0.705	1.373
121	Small	0.743	0.271	2.181	0.246	0.098	0.801	1.622
122	Small	0.865	0.331	2.448	0.387	0.15	0.979	1.286
123	Small	0.445	0.17	1.2	0.13	0.039	0.609	1.105
124	Small	0.909	0.288	2.305	0.209	0.08	0.625	2.182

Volume : 5 | Issue : 10 | October 2015 | ISSN - 2249-555X

125	Small	0.508	0.206	1.44	0.185	0.053	0.97	1.093
126	Small	0.751	0.302	2.218	0.37	0.105	0.69	1.233
127	Small	0.423	0.153	1.099	0.104	0.026	0.831	1.189
128	Small	0.456	0.189	1.398	0.134	0.044	0.976	1.214

Table(4-b): AFM particle analyses for sample M1/1200°C.

Firing temperature (°C)	Mean radius (μm)	Max. diameter (μm)	Volume (nm^3)	Distortion coefficient	Roughness
900	0.41	1.16	0.39	0.81	1.62
1200	0.45	1.30	0.40	0.76	1.87

Table(5): The average values of the surface parameters for mixes M1/900°C and M1/1200°C.

REFERENCE 1-L.M.Levinson and H.R.Philipp. Am.Ceram. Bull.64,639-47 , 1986. 2- G.D.Mahan, L.M.Levinson and H.R.Philipp. J.Appl.Phys. 50,2799,1979. 3- Choon-Woo Nahm. Department of Electrical Engineering, Dongeui University, Busan 614- 714, Republic of Korea. accepted 6 May 2006. 4-Bernik, S. and N. Daneu, 2007. Characteristics of ZnO-based varistor ceramics doped with Al2O3. J. Eur. Ceram. Soc., 27: 3161-3170. 5-Cong, L., X. Zheng, P. Hu and S. Dan-Feng, 2007. Bi2O3 vaporization in microwave-sintered ZnO varistors. J. Am. Ceram. Soc., 90: 2791-2794. 6-Ott, J., A. Lorenz, M. Harrer, E.A. Preissner and C. Hesse, 2001. The influence of Bi2O3 and Sb2O3 on the electrical properties of ZnO-based varistors. J. Electroceram., 6: 135-146. 7-So, S.J. and C.B. Park, 2002. Improvement in the electrical stability of semiconducting ZnO ceramic varistors with SiO2 additive. J. Korean Phys. Soc., 40: 925-929. 8- Choon-W. Nahm. Journal of the American Ceramic Society. Volume 95, Issue 7, pages 2093–2095, July 2012. 9- Schwarzl, T., Heiss, W., Springholz, G., Aigle, M., Pascher, H. 2000, Electron. Lett., 36, 322. 10- Springholz G., Bauer, G. 2007, Phys. Stat. Sol. B, 8, 2752. 11-A. Sedky, T.A. El-Brolossy and S.B. Mohamed. J. Physics and Chemistry of Solids, Volume 73, Issue 3, March 2012, Pages 505–510. 12- S.E. Mansour, O.A. Desouky, S.M. Negim and W.A. Kamil, 2011. Microstructure and Current-voltage Characteristics of (ZnO-CuO) Varistor System in the Presence of Additive Oxides, Cr2O3, Bi2O3 and NiO. Current Research in Chemistry, 3: 29-48.